The influence of austenitization time and temperature on the austenite grain growth in high Ti-V HSLA steels

SRJ Rezaei[1,a,*], CW Siyasiya[1,b], Z Tang[2,c], J Moema[1,3,d]

[1] *Department of Materials Science & Metallurgical Engineering, University of Pretoria, Hatfield, Pretoria, South Africa*
[2] *Department of Materials Science and Engineering, Sichuan University, Chengdu 610000, China*
[3] *Advanced Materials Division (AMD), Mintek, 200 Malibongwe Drive, Randburg, 2125, South Africa*
Email: [a] rezajafarpour2010@gmail.com, [b] charles.siyasiya@up.ac.za , [c] sacdtzh@163.com, [d] josephm@mintek.co.za*

Abstract

Generally, in high titanium-containing high strength low alloy (HSLA) steels, the challenge is to ensure that an adequate amount of Ti dissolves during soaking for precipitate strengthening during cooling or hot working. Therefore, this work focused on the effect of soaking time and temperature on the austenite grain growth kinetics of HSLA steels, of the three alloys containing 0.1 %Ti, and 0 to 0.12 %V. The samples were austenitized at 1150 and 1280 °C for 1, 2 and 3 hrs and quenched in a 10% NaCl brine. Thereafter, the samples were tempered at 490 °C for 72 hrs in order to reveal the prior austenite grain boundaries. The grain size was analysed by the linear intercept method. The precipitation behaviour was predicted by Thermo-Calc software and confirmed by SEM-EDS. At 1150 °C austenitizing temperature, all three steel grades exhibited the Ti (C, N) (Type 1), (Mn-Ti) (C, S) (Type 2), MnS (Type 3), $(Ti_4C_2S_2)$ (Type 4) and TiC (Type 5) precipitates. After escalating the temperature to 1280 °C, only the TiC dissolved. Type 4 and 5 precipitates were the finest and possibly responsible for the grain size refinement. Consequently, alloy 1 with the highest S content of 140 ppm exhibited the finest grain size at both temperatures.

Keywords: Austenitization time, Precipitation, Austenite grain growth, HSLA steels

1. Introduction

High-strength low-alloy (HSLA) steels are a type of low-carbon steel that exhibits combination of high strength, excellent toughness, weldability, and good corrosion resistance.[1,2] Recently, to reduce energy consumption and CO_2 emissions, there has been an increasing demand for lightweight vehicles and, therefore HSLA steels are preferred in the automotive industry for the reduction of vehicle weight.[3] Also, these alloys have been applied to oil and gas transportation, navy vessels, and even nuclear fission power plant components due to their excellent mechanical properties.[2]

To obtain the desired microstructure and mechanical properties Ti, V, Nb, and Mo elements are usually added in small amount for the production of high-strength steels. These elements can improve the strength of steels by grain refining, solid solution, dislocation and precipitation hardening mechanisms.[4-7] Vanadium is commonly preferred to other micro alloying elements additions because of the lower hot working temperatures and rolling forces. Owing to the relatively large solubility of vanadium carbonitride V (C, N), in Ti-V microalloyed steels, it is easier to control precipitation hardening, mainly in the austenite phase at convenient heating temperature.[5] Also, titanium has frequently been added to HSLA steels to enhance the control of austenite grain size during welding or reheating process. Multi-microalloying can, thus, lead to the formation of complex inter metallic precipitates, which can influence the mechanical properties of the HSLA steels.[8]

The precipitation of the carbonitrides is an important phenomenon influencing the microstructure of HSLA steels and the Subsequent mechanical properties.[9] These carbonitrides influence the

evaluation of the austenite grain size during thermomechanical processing, which in turn influence the final microstructure. Hence several studies have been done on precipitation and austenite grain size during hot processing of these steels. The influence of niobium on austenite grain size was studied by K. A. Annan et al.[10] the results showed that there is a linear relationship between Nb content and the activation energy for grain growth. Beata Białobrzeska et al.[11] showed that the austenite grain size has a strong influence on the mechanical properties of the steel.

Under this background, it is necessary to study austenite grain size and precipitation behaviour to design a suitable thermomechanical treatment for the achievement of desired properties at room temperature. This research investigates the effect of austenitization temperature and soaking time on precipitation behaviour and austenite grain size in Ti-V steels.

2. Experimental

The chemical composition of investigated steels are given in Table 1. The steels were machined into 10 mm × 15 mm (diameter × length) cylindrical specimens. These specimens were austenitised at 1150 and 1280°C and soaked for 1, 2 and 3 hrs, and then quenched in brine with 10% NaCl.

The quenched specimens were halved along the longitudinal axis and one half was tempered at 490 °C for 72 hrs to improve the response of prior austenite grain boundaries etching. The tempered samples were mounted, ground, polished and then etched with $FeCl_3$ solution containing 5g iron chloride, 100 ml distilled water and 5 drops of hydrochloric acid. Etching was carried out at room

Table 1: chemical composition of the experimental steel (mass. %)

Alloy	C	Mn	Ti	Si	N	S	Al	Cr	V	P	Fe
Alloy 1	0.112	1.67	0.082	0.43	0.0054	0.014	0.006	0.659	0.12	0.008	balance
Alloy 2	0.115	1.48	0.081	0.416	0.0043	0.006	0.01	0.631	0.06	0.008	balance
Alloy 3	0.108	1.52	0.099	0.43	0.0043	0.006	0.015	0.613	---	---	balance

temperature for times ranging from 10 to 30 minutes. The samples were observed under an Olympus BX51MTM optical microscope to reveal the prior austenite grain boundaries. The austenite grain size was measured using the average linear intercept method.

A JSM-IT300 JEOL scanning electron microscopy (SEM) equipped with energy dispersive spectroscopy (EDS) was employed to determine the precipitate's composition and morphology. Thermo-Calc software was used to predict the precipitation behaviour.

3. Results and discussion

The volume fraction of precipitates and solubility of alloy element as function of temperature are shown in Figures 1 and 2. The
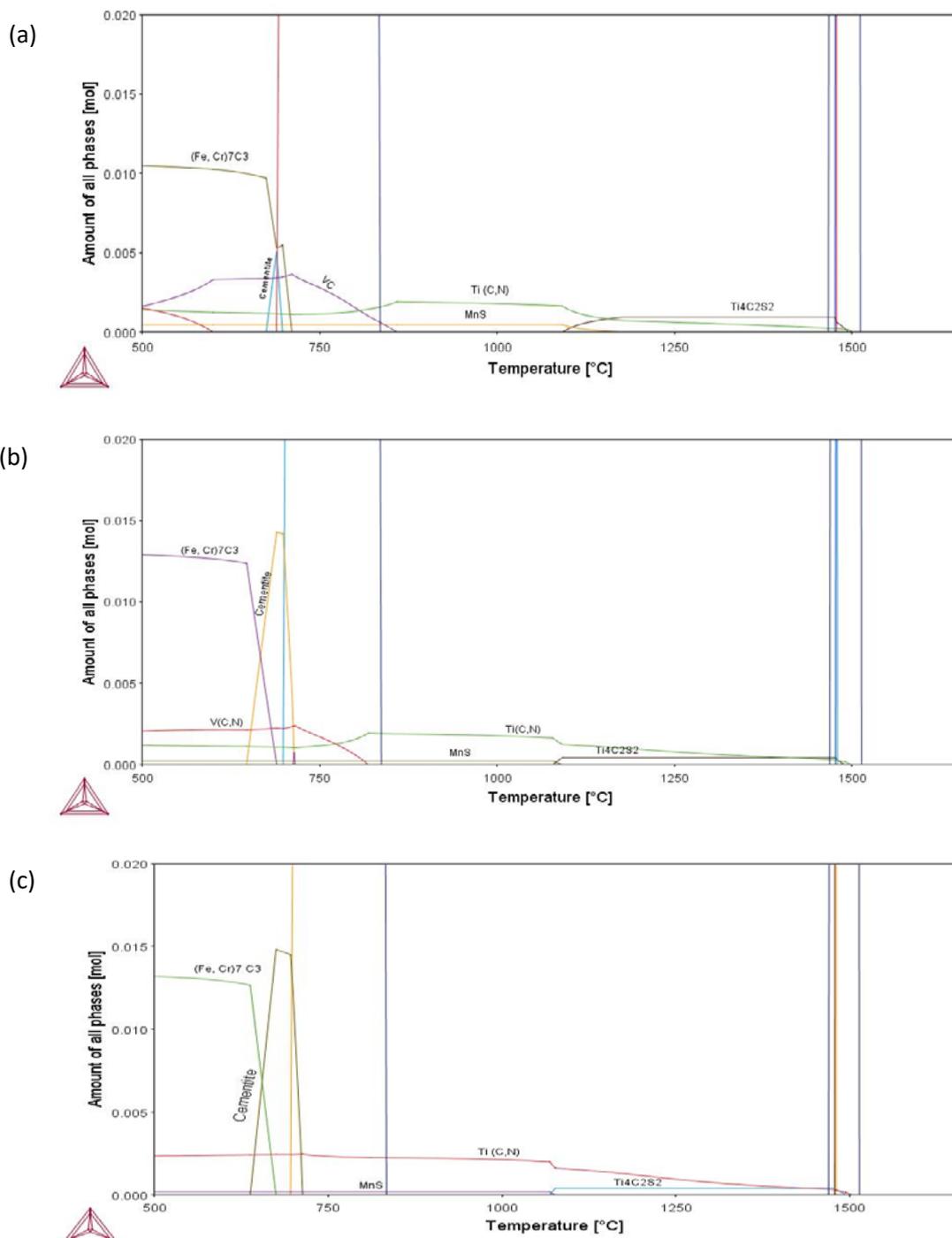

Figure 1: Thermo-Calc predictions of precipitates formation (a) alloy 1 (b) alloy 2 (c) alloy 3
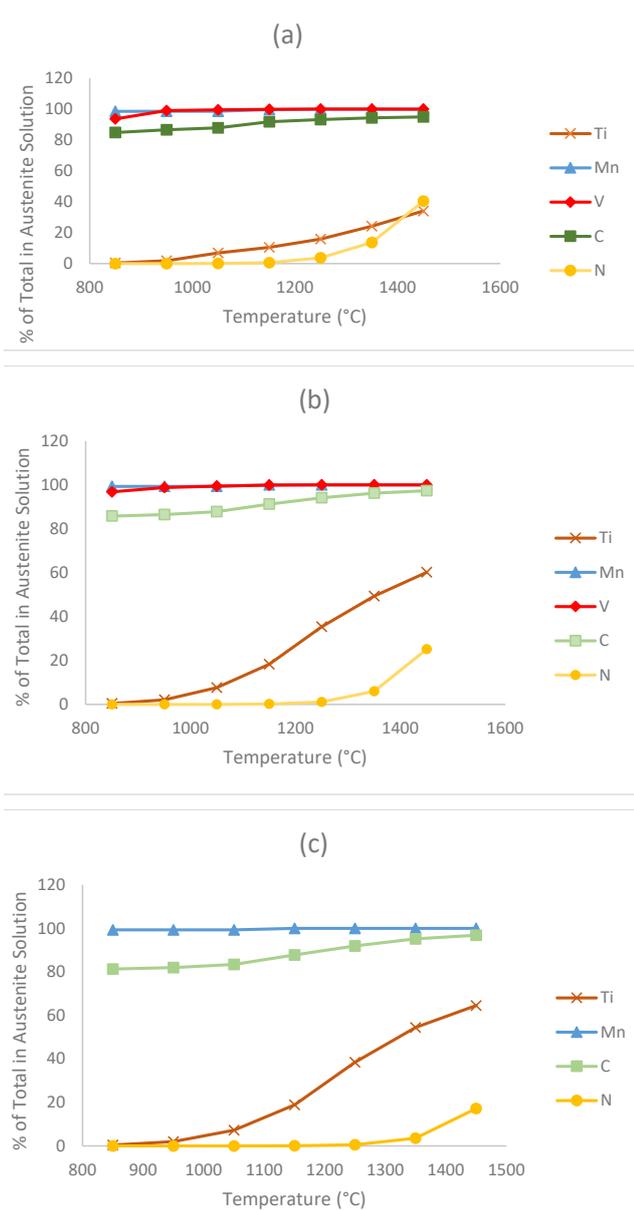
Figure 2: Solubility of alloy elements in austenite phase (a) alloy 1 (b) alloy 2 (c) alloy 3

Thermo-Calc predictions show that VC and MnS completely dissolve at a reheating temperature around 850 and 1100 °C respectively, but Ti (C, N) particles are stable at this temperature and also $Ti_4C_2S_2$ begin to form at temperature higher than 1100 °C during the austenitization process. In other words, TiN precipitates normally form in the melt prior to solidification.[12] These particles are thermodynamically stable in austenite and ferrite and, therefore, would not dissolve during soaking or hot rolling furthermore. The Thermo-Calc predictions also revealed that, unlike the rest of the steels, only alloy 1 would form substantial amount of MnS particles due to the higher amount of S. It was also the alloy that was predicted to have the least amount of Ti in solution, Figure 2.

Figure 3 reveals the morphology of the Ti (C, N) and Al_2O_3 particles, whereby the latter acted as a preferential nucleation site. In other words, a cleaner steel would promote the Ti to remain in solution during solidification process as desired. In addition, MgO/MgS and MnS also expedited the heterogeneous nucleation of the Ti (C, N) because the required undercooling energy is much lower than that for the homogeneous nucleation.[13]

Figures 4 and 5 show the morphology, distribution and composition of precipitates of as-quenched alloy 1 after austenitization at 1150 and 1280 °C respectively.

As may be seen from Figure 4, there were 5 different types of precipitates at 1150 °C reheating temperature. Type 1 precipitates were cuboidal titanium carbonitrides (Ti (C, N)). Type 2 precipitates were the medium size manganese-titanium carbosulfides ((Mn-Ti) (C, S)). Type 3 precipitates were the manganesesulfides (MnS). Type 4 and 5 precipitates were the fine spherical titanium carbosulfide ($Ti_4C_2S_2$) and titanium carbide (TiC) respectively.

The only particles that dissolved at 1280 °C were the TiC while the rest remained, Figure 5, and this was agreement with the Thermo-Calc prediction.

Figures 6 and 7 show the optical micrograph of the prior austenite grain for the three investigated alloys after austenitization at 1150 and 1280 °C for 2 hr. The austenite grain size distribution at 1150 and 1280 °C for various soaking time is shown in Figures
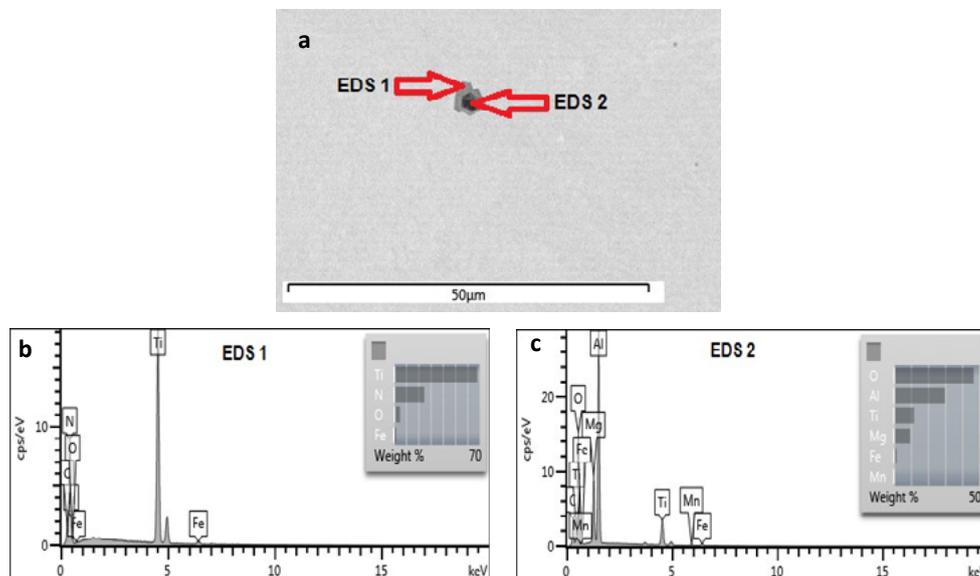

Figure 3: Morphology of Ti (C, N) particles in alloy 3 at 1280 °C after 1 hr, a) SEM- BEI of Ti (N, C), and Al_2O_3, b) Ti (C, N), c) Al_2O_3 EDS spectra
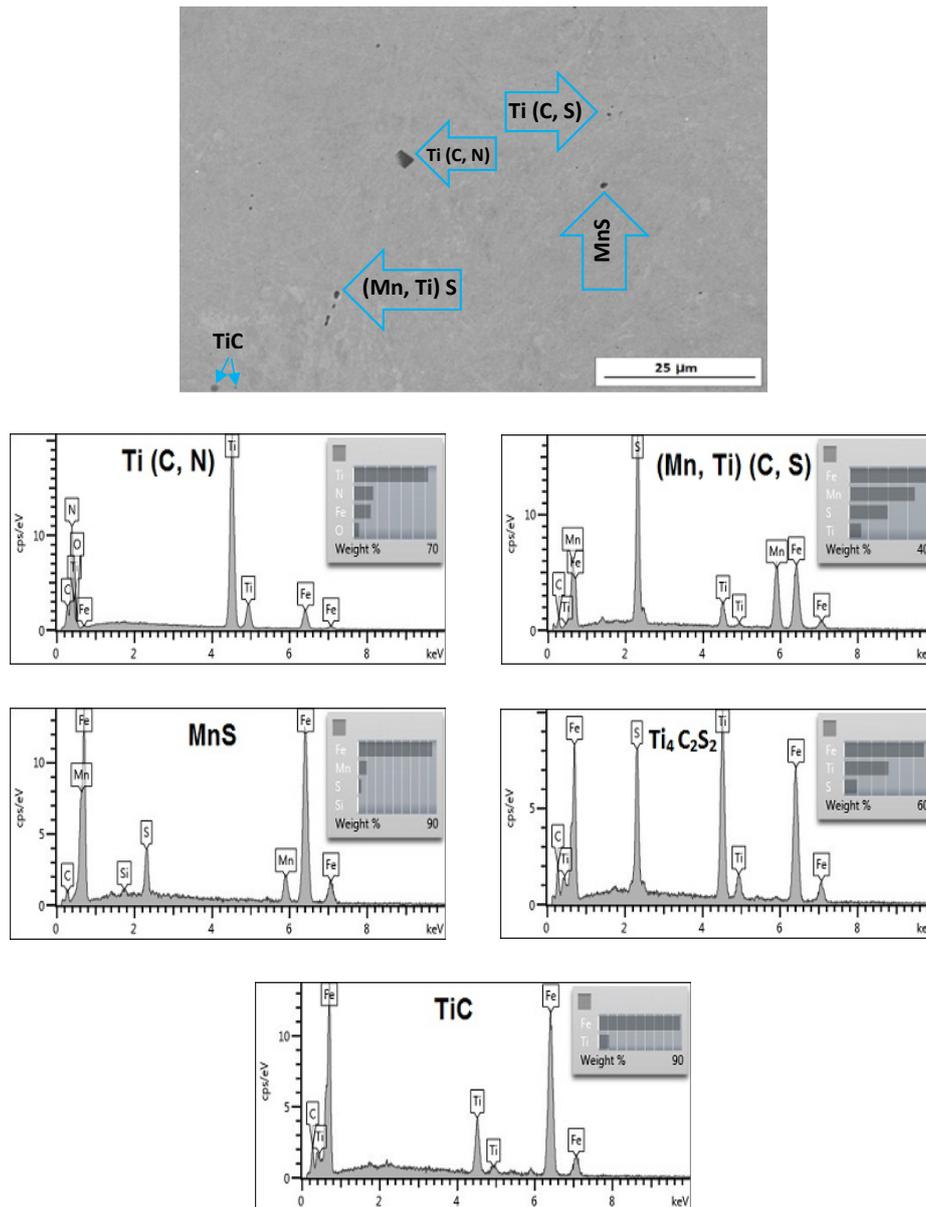
Figure 4: SEM images and EDS spectra for alloy 1 at 1150°C and soaking time 1 hr

8 and 9 respectively. It can be seen that the austenite grain size coarsened with increasing reheating temperature and soaking time. The variation of the austenite grain size with soaking time is summarized in Figures 10 and 11. It is evident that the finer grain size was observed in the steel containing the highest content of V and S of 0.12 and 0.014 mass.% respectively. Therefore, the fine spherical titanium carbosulfide ($Ti_4C_2S_2$) and titanium carbide (TiC) precipitates' volume fraction was highest in alloy 1 and possibly responsible for the grain size refinement, that is, besides the VN particles that could not be observed by SEM. Therefore, it was not surprising that alloy 1 with the highest V and S content exhibited the finest grain size at both temperatures.

The basic relationship of the pinning force of grain boundaries as a function of the particle size and volume fraction is defined by Zener:[10]

$$F_P = \frac{3.\gamma.V_v}{2r} \qquad \text{eq. 1}$$

Where ɣ is the austenite interface energy, V_v is the particle volume fraction, r is average radius of particles.

During austenitization, the precipitates can either dissolve or coarsen depending on the austenitization temperature.[2] Therefore, it is not surprising that the rate of grain growth increases with the soaking temperature. Besides that, the grain growth is a diffusion controlled process and, therefore, its rate increases with an increase in temperature. In this work, it was found that the fine TiC particles were the ones that dissolves as the temperature increases rendering the steel no inhibition to grain growth as the rest of the particles only coarsened.

Figure 12 shows the variation of the Ti (C, N) with the isothermal holding time. While the particle size seemed to increase slightly with an isothermal holding time at 1150 °C. On the contrary, particle size decreased substantially with an isothermal holding time at 1280 °C. This suggests partial dissolution of the Ti (C, N)
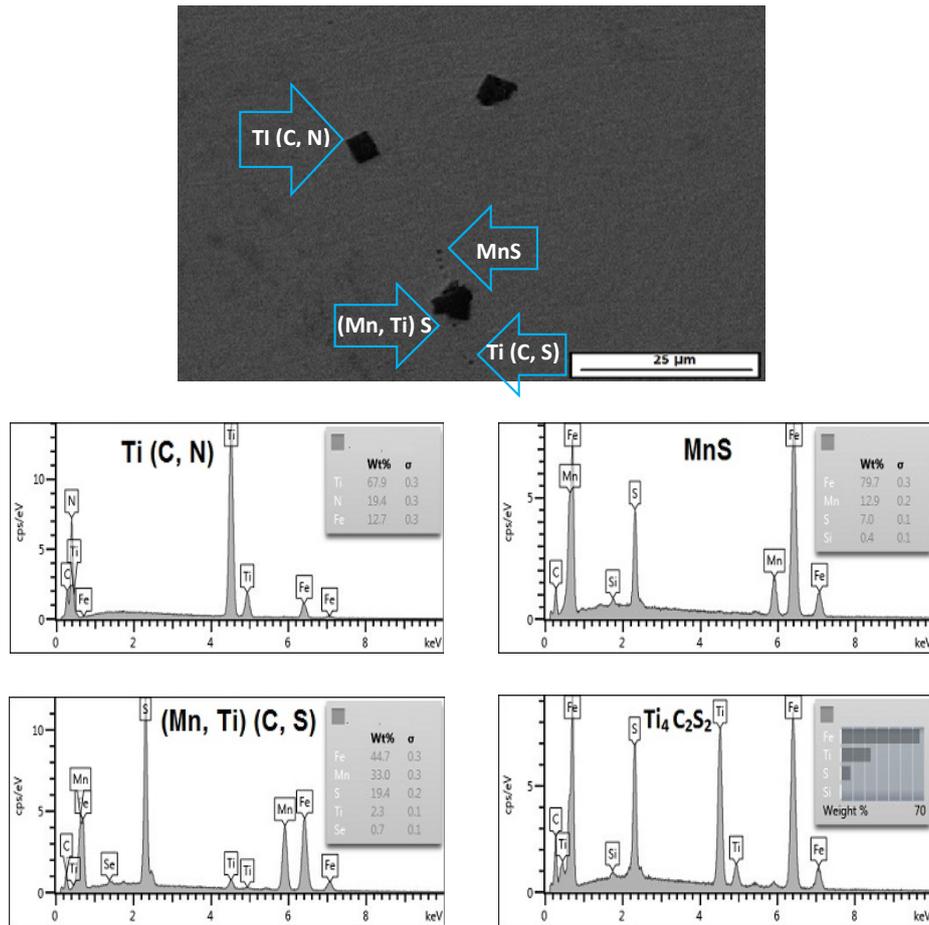
Figure 5: SEM images and EDS spectra for alloy 1 at 1280°C and soaking time 1 hr
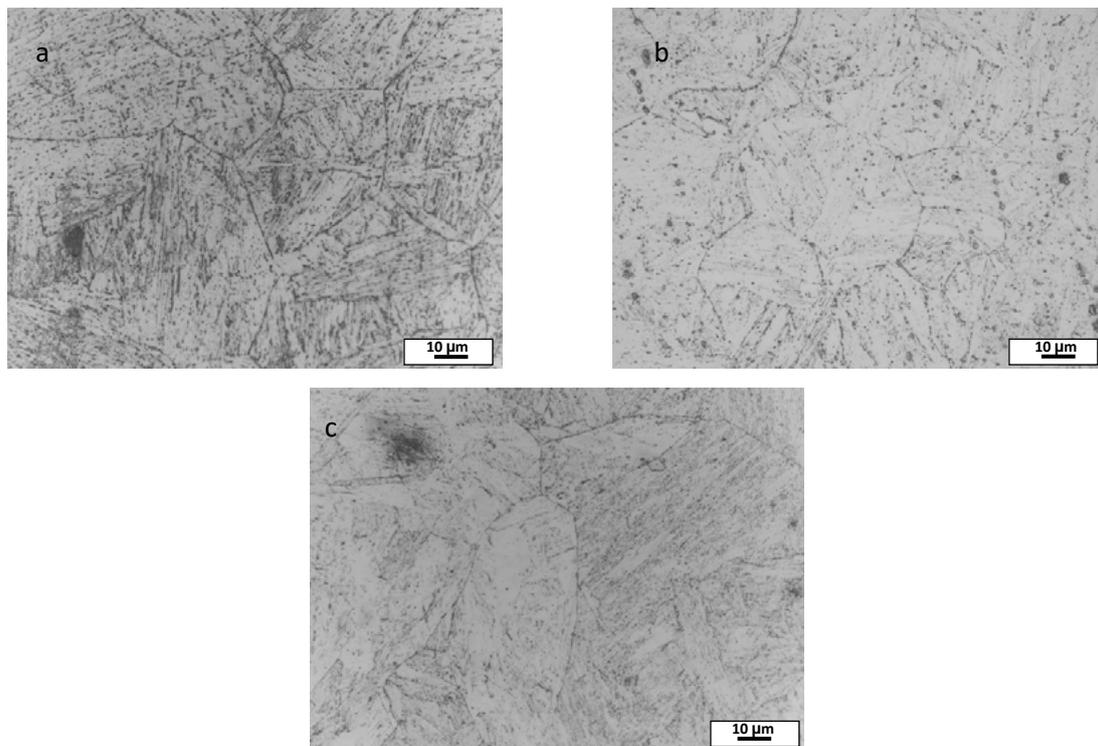

Figure 6: Micrograph showing prior austenite grains at 1150 °C and after 2 hr, a) alloy 1, b) alloy 2, and c) alloy 3
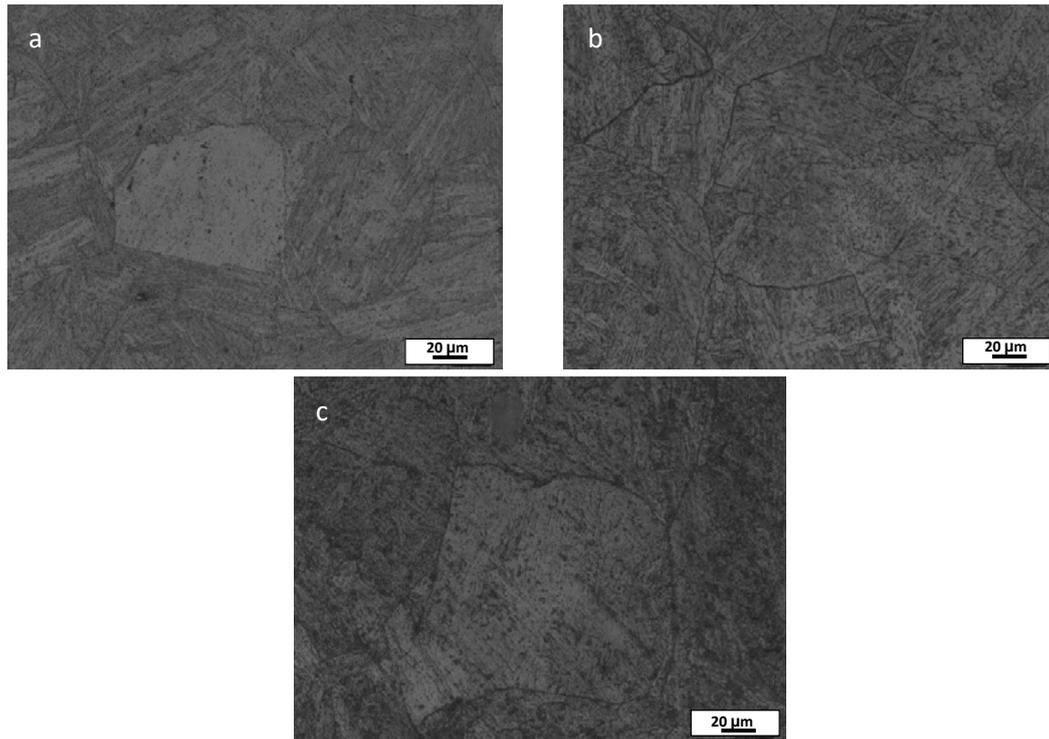
Figure 7: Micrograph showing prior austenite grains at 1280 °C and after 2 hr, a) alloy 1, b) alloy 2, and c) alloy 3
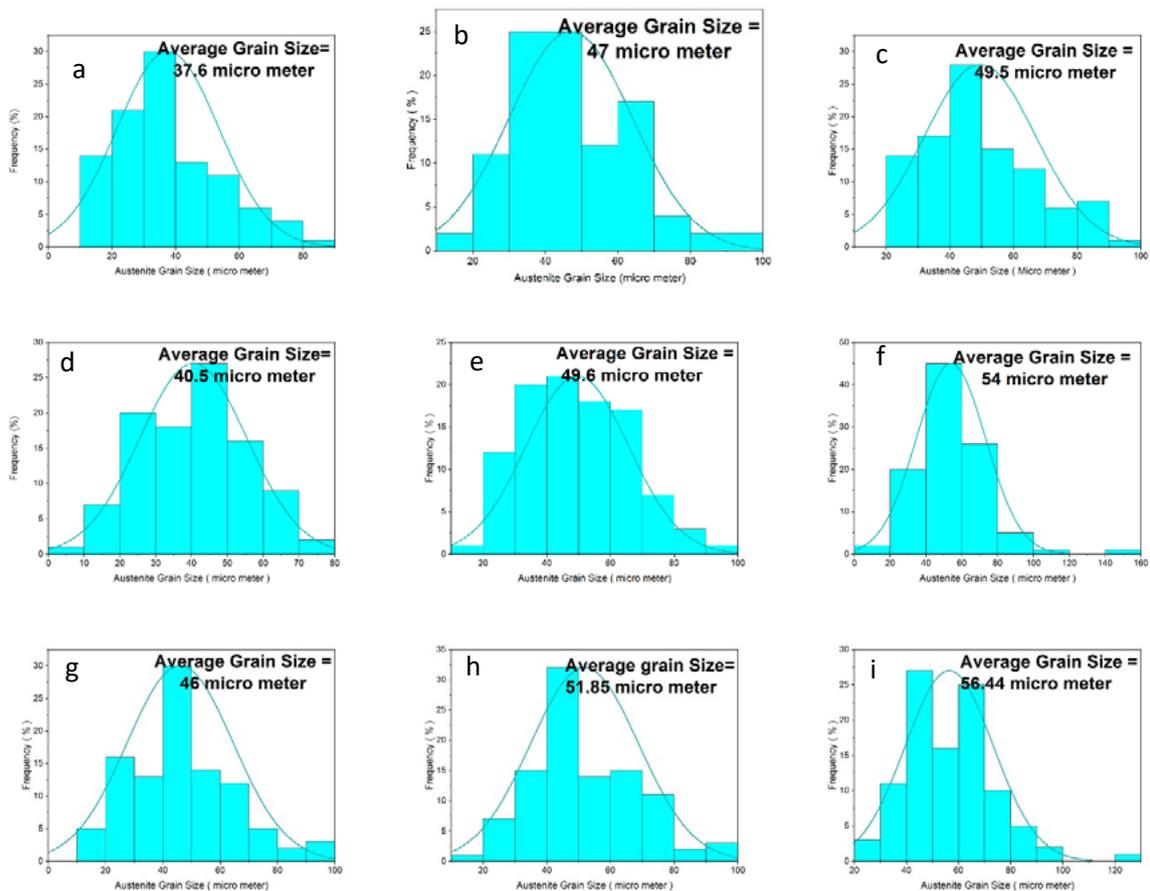

Figure 8: Distribution of prior austenite grain size at austenitization temperature 1150 °C, a) alloy 1 after 1 hr, b) alloy1 after 2 hr, c) alloy 1 after 3 hr, d) alloy 2 after 1 hr, e) alloy 2 after 2 hr, f) alloy 2 after 3 hr, g) alloy 3 after 1 hr, h) alloy 3 after 2 hr, and i) alloy 3 after 3 hr
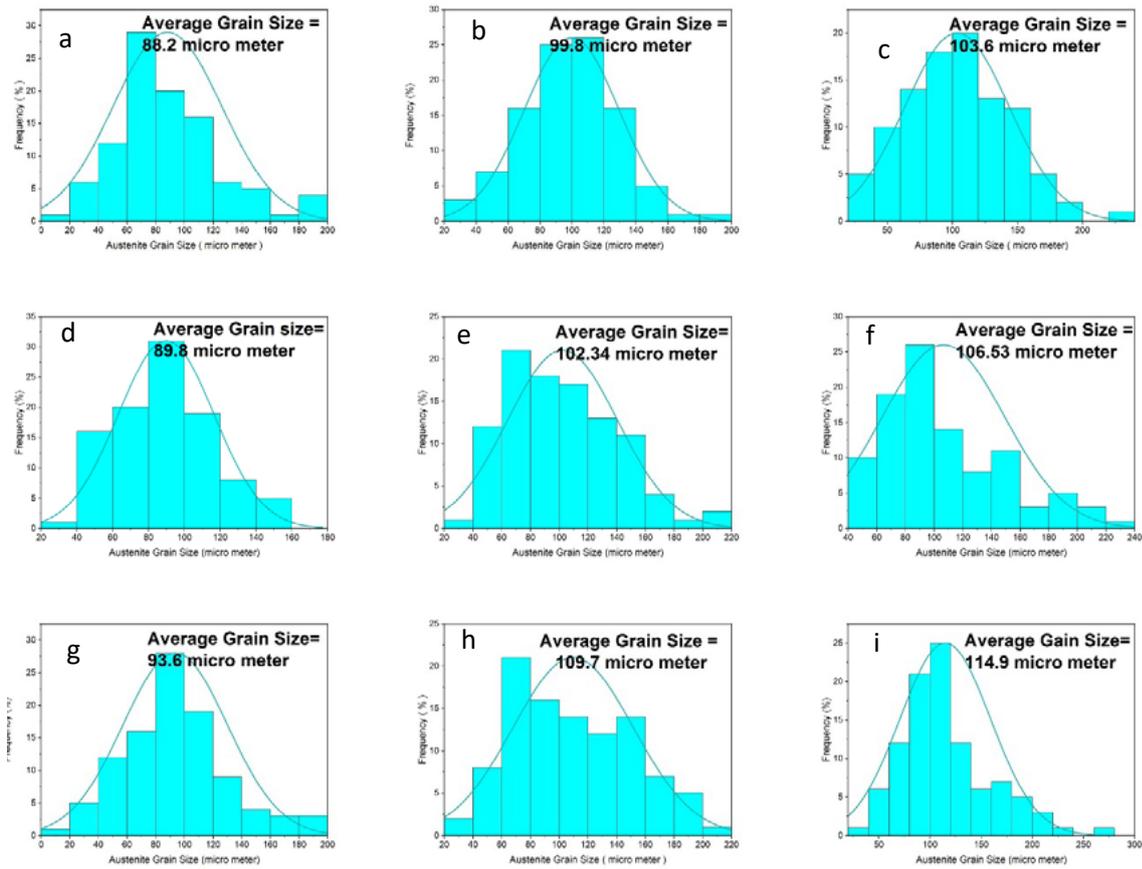
Figure 9: Distribution of prior austenite grain size at austenitization temperature 1280 °C, a) alloy 1 after 1 hr, b) alloy1 after 2 hr, c) alloy 1 after 3 hr, d) alloy 2 after 1 hr, e) alloy 2 after 2 hr, f) alloy 2 after 3 hr, g) alloy 3 after 1 hr, h) alloy 3 after 2 hr, and i) alloy 3 after 3 hr
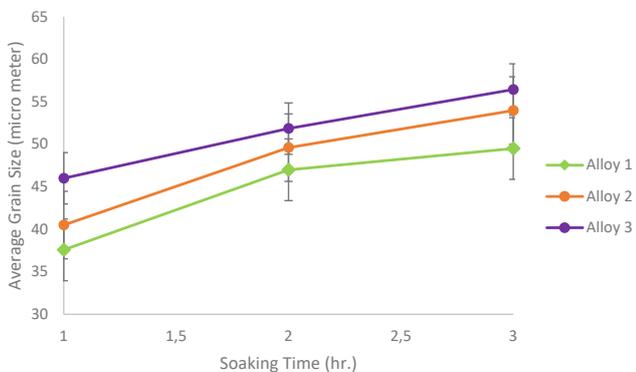

Figure 10: Variation of austenite grain size with holding time at reheating temperature of 1150 °C
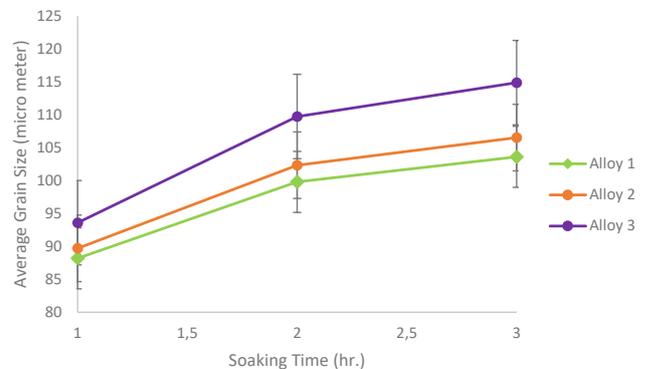

Figure 11: Variation of austenite grain size with holding time at reheating temperature 1280 °C

at 1280 °C as opposed to at 1150 °C. This agrees with the Thermo-Calc prediction, Figure 1.

Conclusions

The influence of the austenitization time and temperature on the precipitation behaviour and austenite grain growth in high Ti-V HSLA steels were investigated and the following conclusions can be made:

- In the investigated steels of high Ti (0.1 mass. %) V (up to 0.12 mass. %) steels, five types of precipitates were observed namely; Type 1 precipitates (Ti (C, N)), Type 2 precipitates ((Mn-Ti) (C, S)), Type 3 precipitates (MnS), Type 4 precipitates ($Ti_4C_2S_2$) and Type V precipitates (TiC).
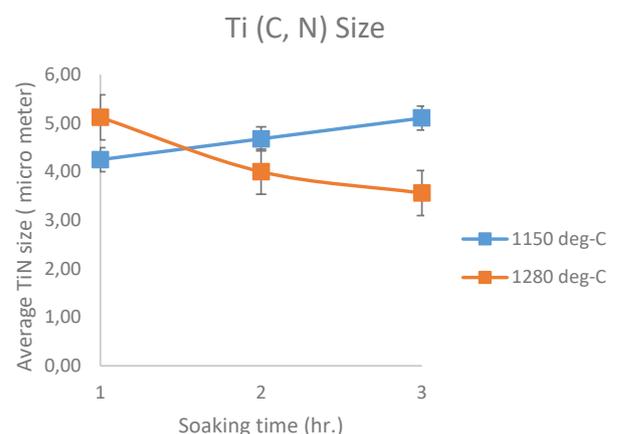

Figure 12: Variation of Ti (C, N) size for alloy 1 at reheating temperatures of 1150 and 1280 °C

- The fine type 5 Precipitates (TiC) completely dissolve into austenite by increasing the reheating temperature to 1280 °C. This led to substantial grain growth since the rest of the precipitates remained coarser.

- The Al_2O_3 inclusions acted as preferential nucleation sites for the Ti (C, N) particles. This suggested that probably a cleaner steel would promote the Ti to remain in solution during the solidification process. In other words, this would promote precipitation of the finer TiC for grain refinement in this grade of steel.

Reference

1. Xiao W, Zuo-cheng W, Xie-bin W, Yi-ran W, Jun-qing G, Xiu-ling Z. 2012. Effect of Cooling Rate and Deformation on Microstructures and Critical Phase Transformation Temperature of Boron-Nickel Added HSLA H-Beams. Journal of Iron and Steel Research 19 (2), 62-66.

2. Yang Zhang, Xiaohua Li, Yongchang Liu, Chenxi Liu, Ji Dong, Liming Yu, Huijun Li. 2020. Study of the kinetics of austenite grain growth by dynamic Ti-rich and Nb rich carbonitride dissolution in HSLA steel: In-situ observation and modelling. Materials Characterization 169, 110612.

3. Xukai Zhang, Chrysoula Ioannidou, Gret H.ten Brink, Alfonso Navarro-Lopez, Jan Wormann, Jean Campaniello, Robert M. Dalglieshh, Ad A. van Well, S. Erik Offerman, Winfried Kranendonk, Bart J. Kooi. 2020. Microstructure, precipitate and property evolution in cold-rolled Ti-V high strength low alloy steel. Materials and Design 192, 108720.

4. Ji Dong, Chenxi Liu, Yongchang Liu, Xiaosheng Zhou, Qianying Guo, Huijun Li. 2017. Isochronal phase transformation of Nb–V–Ti microalloyed ultra-high strength steel upon cooling. Fusion Engineering and Design, 125, 423–430.

5. Weijun Hui, Yongjian Zhang, Chengwei shao, Silian Chen, Xiaoli Zhao, Han Dong. 2016. Effect of Cooling Rate and Vanadium Content on the Microstructure and Hardness of Medium Carbon Forging Steel. Journal of Materials Science & Technology, 32, 545–551.

6. Jun Chen, Shuai Tang, Zhenyu Liu, Guodong Wang. 2013. Influence of molybdenum content on transformation behavior of high performance bridge steel during continuous cooling. Materials and Design, 49, 465–470.

7. Yong Tian, Qun Li, Zhao-dong Wang, Guo-dong Wang. 2015. Effects of Ultra Fast Cooling on Microstructure and Mechanical Properties of Pipeline Steels. Journal of Materials Engineering and Performance, 24, 3307–3314.

8. Hyun Jo Jun, K.B. Kang, C.G. Park. 2003. Effects of cooling rate and isothermal holding on the precipitation behavior during continuous casting of Nb–Ti bearing HSLA steels. Scripta Materialia. 49, 1081–1086.

9. Suman K. Mishra, S. S. Das, S. Rangagathan. 2002. Precipitation in high strength low alloy (HSLA) steel: a TEM study. Materials Science and Engineering, A323, 285–292.

10. K. A. Annan, C. W. Siyasiya, W. E. Stumpf. 2015. The influence of niobium content on austenite grain growth in microalloyed steels. The Journal of the Southern African Institute of Mining and Metallurgy, 115, 973-980.

11. Beata Białobrzeska, Lukasz Konat, Robert Jasinski. 2017. The Influence of Austenite Grain Size on the Mechanical Properties of Low-Alloy Steel with Boron. Metals, 7, 26, 1-20.

12. M. Charleux, W. J. Poole, M. Militzer, A. Deschamps. 2001. Precipitation Behavior and Its Effect on Strengthening of an HSLA-Nb/Ti Steel. Metallurgical and Materials Transactions A, 32A, 1635-1647.

13. Wen Liang, Qing Yuan, Qingxiao Zhang, Wenwei Qiao. 2021. Study on Fraction Mechanism and Microstructural Evolution in 780 MPa Grade FB Steel with a High hole Expanding Ratio. Journal of materials engineering and Performance, 30(3), 1641-1651.